VIII. QCD, jets and gluons

- *Quantum Chromodynamics (QCD)*: the theory of strong interactions
  - Interactions are carried out by a <u>massless</u> spin-1 particle – *gauge boson*
  - In quantum electrodynamics (QED) gauge bosons are photons, in QCD – *gluons*
  - Gauge bosons couple to conserved charges: photons in QED – to electric charges, and gluons in QCD – to colour charges (I_3^C and Y^C)
- Gluons have electric charge of 0 and couple only to colour charges $\Rightarrow$ strong interactions are **flavour-independent**, same for u,d,s,c,b and t

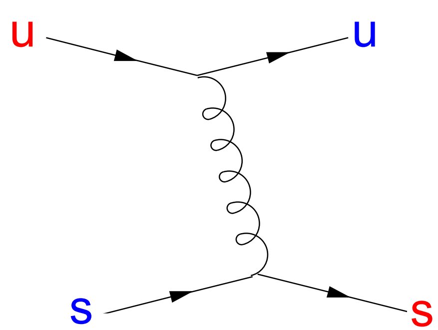

Figure 112: Gluon exchange between quarks: colour charges must be conserved, hence the gluon must carry a colour (r) and an anticolour ($\bar{b}$)

❖ Gluons carry colour charges themselves!

Colour quantum numbers are conserved ⇒ for the gluon on Figure 112:

$$I_3^C = I_3^C(r) - I_3^C(b) = 1/2 - 0 = 1/2 \qquad (126)$$

$$Y^C = Y^C(r) - Y^C(b) = 1/3 - (-2/3) = 1 \qquad (127)$$

There are 8 different colour states of gluons (χ_{gi}^C - color wave function):

Gluon colour wavefunction χ_{gi}^C	I_3^C	Y^C
$\chi_{g1}^C = r\bar{g}$	1	0
$\chi_{g2}^C = \bar{r}g$	-1	0
$\chi_{g3}^C = r\bar{b}$	1/2	1
$\chi_{g4}^C = \bar{r}b$	-1/2	-1
$\chi_{g5}^C = g\bar{b}$	-1/2	1
$\chi_{g6}^C = \bar{g}b$	1/2	-1
$\chi_{g7}^C = (g\bar{g} - r\bar{r})/\sqrt{2}$	0	0
$\chi_{g8}^C = (g\bar{g} - r\bar{r} - 2b\bar{b})/\sqrt{6}$	0	0

Gluons hence can couple to other gluons!

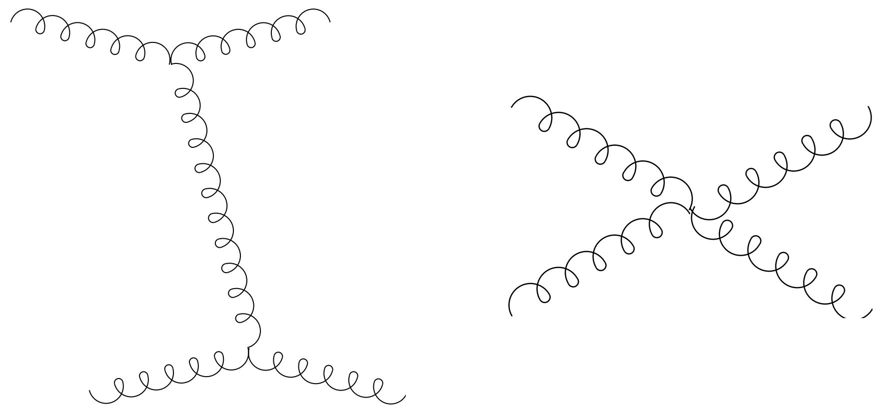

Figure 113: Lowest-order contributions to gluon-gluon scattering

- Gluons carry colours and can not exist as free particles
- Bound colourless states of gluons are called *glueballs* (not detected experimentally yet)
- Gluons are massless $\Rightarrow$ long-range interaction (still, not free particles, unlike γ)

Principle of *asymptotic freedom* (1973 - Gross, Politzer, Wilczek):

- At short distances between particles, strong interactions are sufficiently weak (lowest order diagrams) $\Rightarrow$ quarks and gluons are essentially free particles
- At large distances, high-order diagrams dominate $\Rightarrow$ many coloured objects, "anti-screening" of colour charge $\Rightarrow$ interaction is very strong

Asymptotic freedom thus implies the requirement of colour confinement

- Due to the complexity of high-order diagrams, the very process of confinement can not be calculated analytically $\Rightarrow$ only numerical models can be used

Strong coupling constant α_s

Constant α_s is QCD analogue of α_{em} - measure of interaction strength

- α_s is a "*running constant*": it increases with increase of r, becoming divergent at very big distances

At short distances, quark-antiquark potential is:

$$V(r) = -\frac{4}{3}\frac{\alpha_s}{r} \qquad (r < 0.1 fm) \tag{128}$$

At large distances, quarks are subject to the "*confining potential*" which grows with r:

$$V(r) \approx \lambda r \qquad (r > 1 fm) \tag{129}$$

Quark-antiquark potential

In a simplified manner, quark-antiquark potential can be illustrated as:

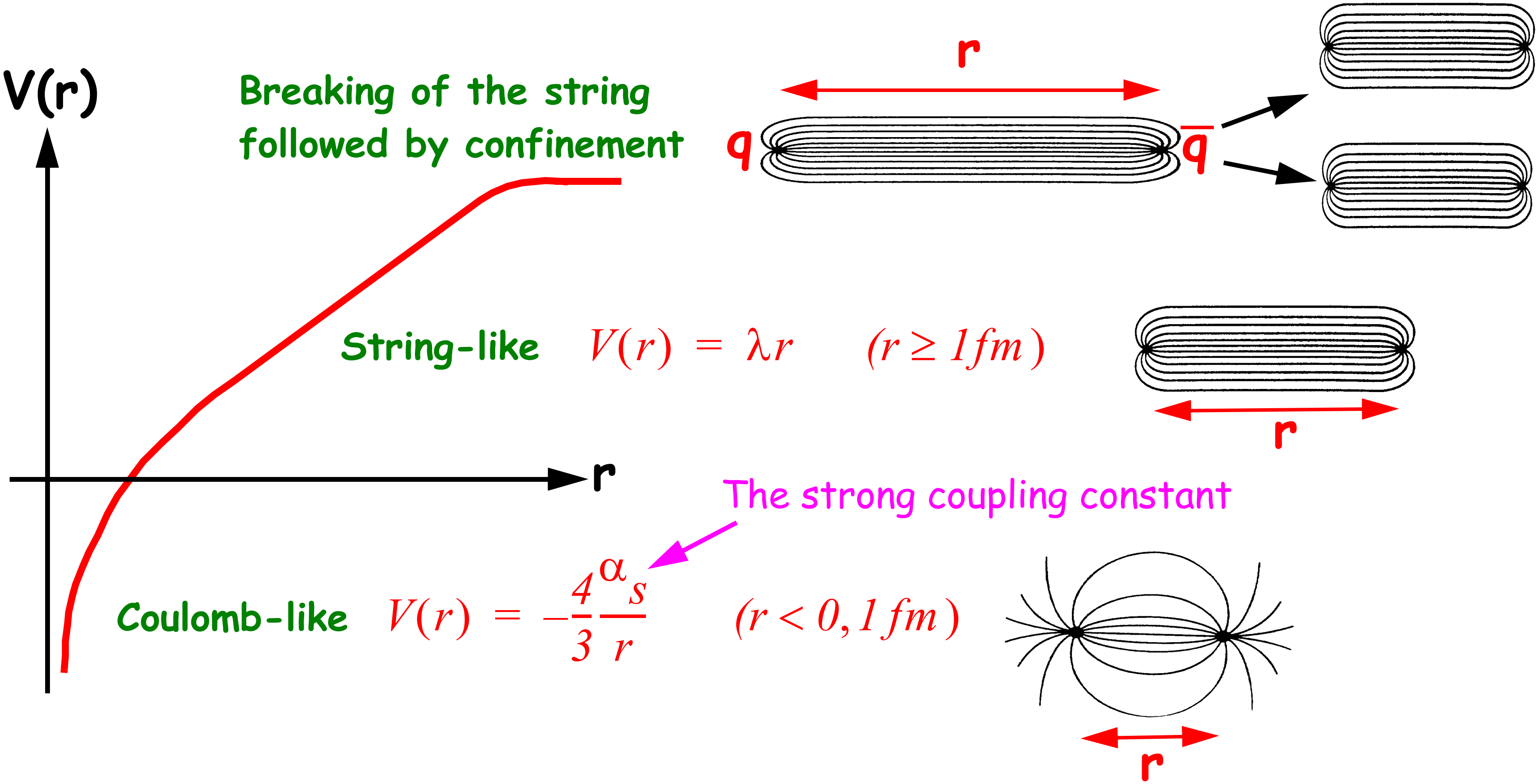

In QCD, Lorentz-invariant energy-momentum transfer Q is used to characterize interactions

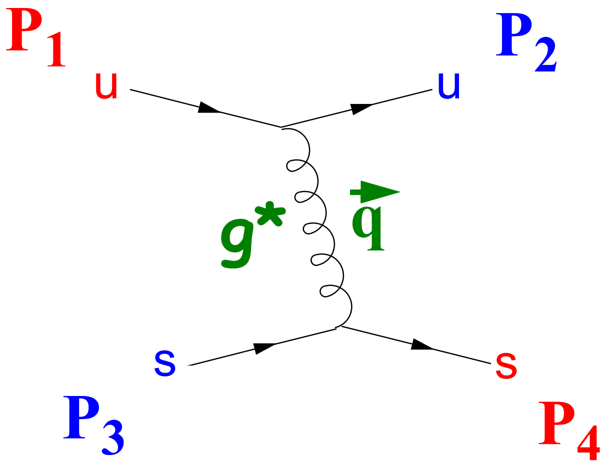

The 4-momenta of the quarks are:

$$P = (E,\bar{p}) = (E, p_x, p_y, p_z)$$

The 4-vector energy-momentum transfer Q ("invariant mass" of the gluon) is defined as:

$$Q^2 = - q \cdot q$$

where q is calculated from 4-momenta of the quarks:

$$q = (E_q,\bar{q}) = P_1 - P_2 = (E_1 - E_2, \bar{p}_1 - \bar{p}_2)$$

- **Short** distance interactions are associated with the **large** momentum transfer $\bar{q}$ between the particles:

$$\left|\vec{q}\right| = O(r^{-1}) \tag{130}$$

- α_s is <u>decreasing</u> with increasing momentum transfer Q^2

In the *leading order* of QCD, α_s dependency on Q is given by

$$\alpha_s = \frac{12\pi}{(33-2N_f)\ln(Q^2/\Lambda^2)} \tag{131}$$

Here N_f is the number of allowed quark flavours, and $\Lambda \approx 0.2$ GeV is the QCD scale parameter which has to be defined experimentally.

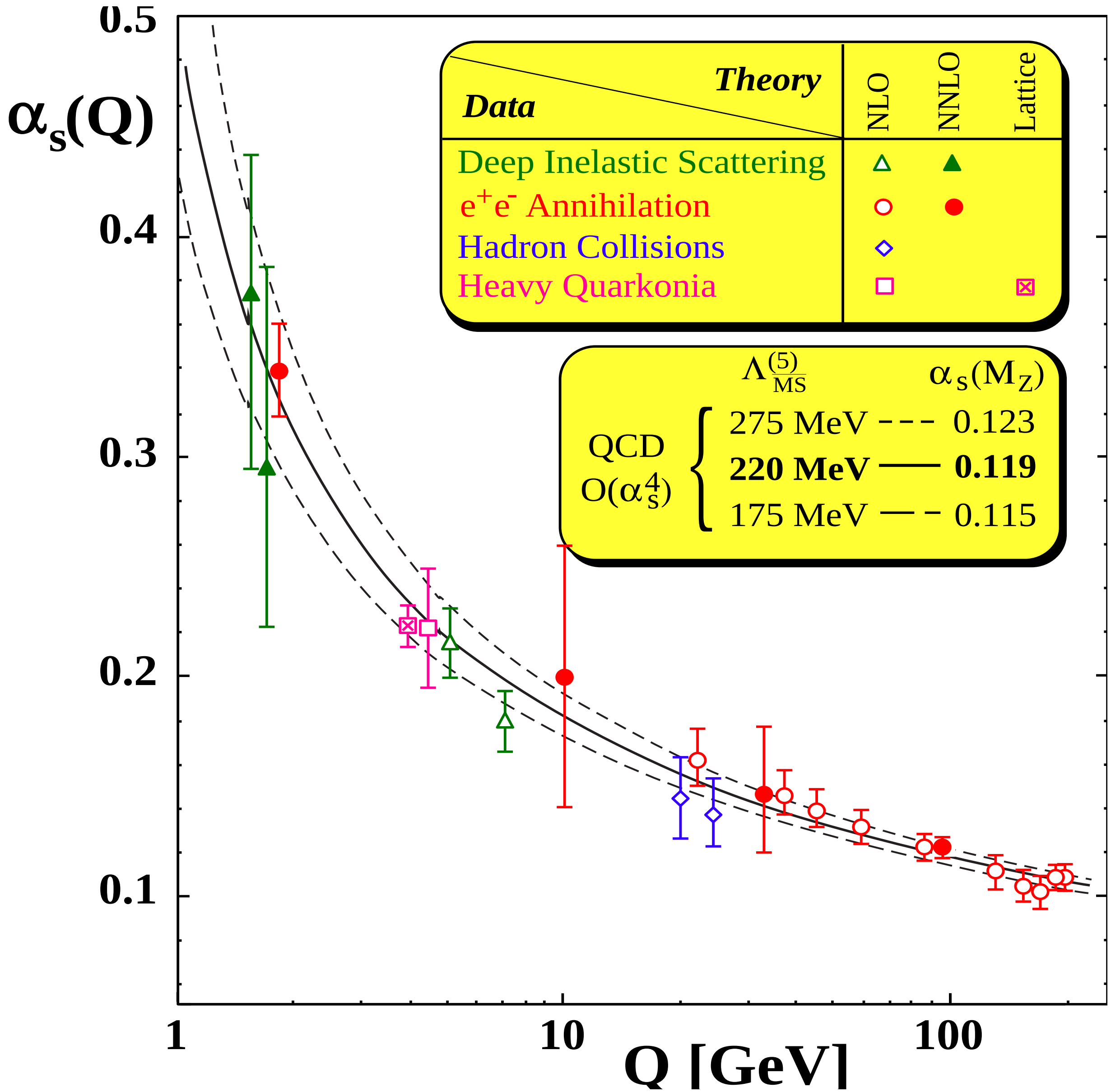

Figure 114: Running of α_s, experimental data vs theory

Electron-positron annihilation

- A perfect laboratory for precision studies of quarks and gluons:

$$e^+ + e^- \to \gamma^*/Z \to \text{hadrons} \qquad (132)$$

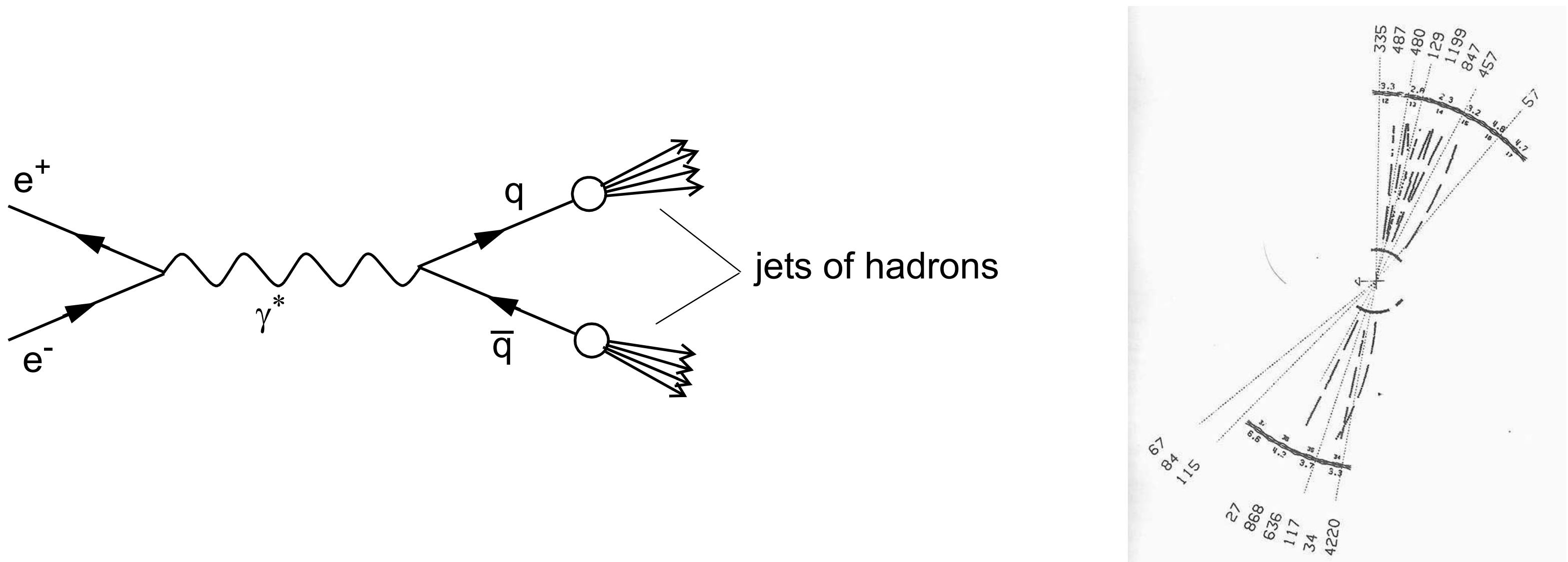

Figure 115: e^+e^- annihilation into hadrons (JADE experiment display, 1979 - first “trace” of quarks fragmenting into jets of hadrons)

- At energies between ~12 GeV and ~45 GeV per beam, e^+e^- annihilation produces a photon which converts into a quark-antiquark pair
- At centre-of-mass energies around Z boson mass, the process goes via Z

Most QCD studies were done at PETRA (1980ies) and LEP (1990ies) e^+e^- colliders at DESY and CERN, respectively:

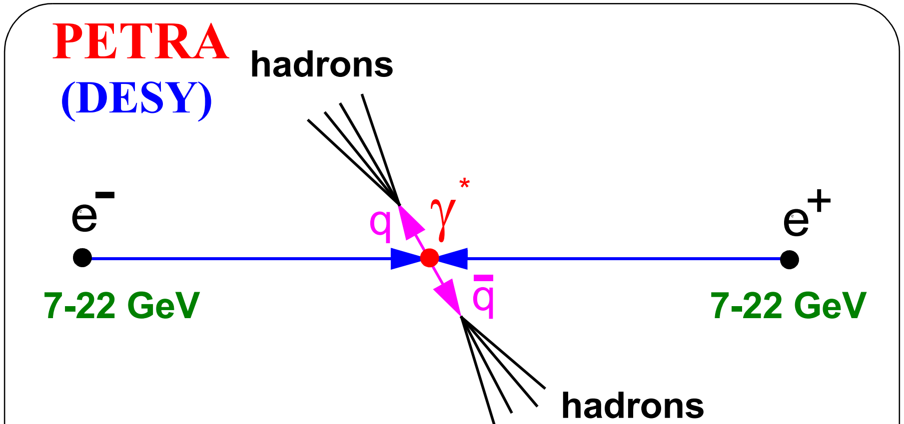

Length: 2.3 km
Experiments: Tasso, Jade, Pluto, Mark J, Cello

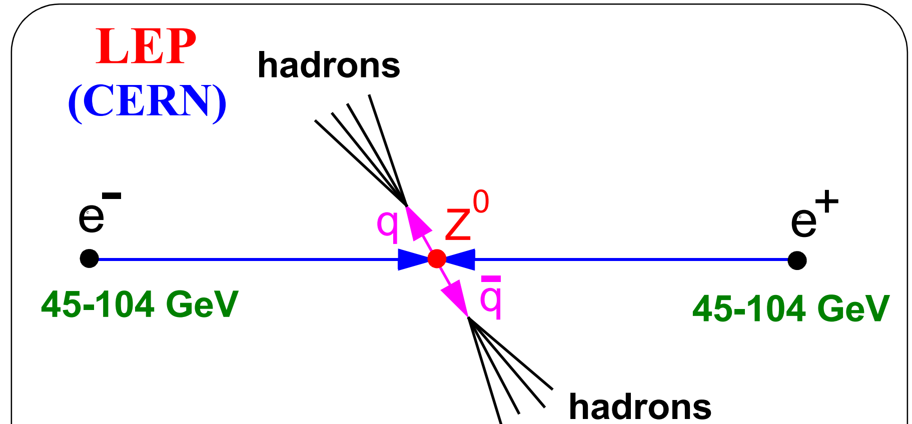

Length: 27 km (4184 magnets)
Experiments: DELPHI, OPAL, ALEPH, L3

- Quark and antiquark *fragment* into observable hadrons
- When beam energies are equal, quark and antiquark momenta are equal and counterparallel $\Rightarrow$ hadrons are produced in two opposing *jets* of equal energies
- Direction of a jet reflects direction of a corresponding quark

Compare the process (132) with the reaction

$$e^+ + e^- \rightarrow \gamma^*/Z \rightarrow \mu^+ + \mu^- \tag{133}$$

Angular distribution of muons (spin 1/2) can be calculated as:

$$\frac{d\sigma}{d\cos\theta}(e^+e^- \rightarrow \mu^+\mu^-) = \frac{\pi\alpha^2}{2Q^2}(1 + \cos^2\theta) \tag{134}$$

where θ is the production angle with respect to the initial electron direction in center-of-mass frame.

If quarks, like muons, have spin 1/2, angular distribution of jets goes like $(1 + \cos^2\theta)$; if quarks have spin 0 – like $(1 - \cos^2\theta)$

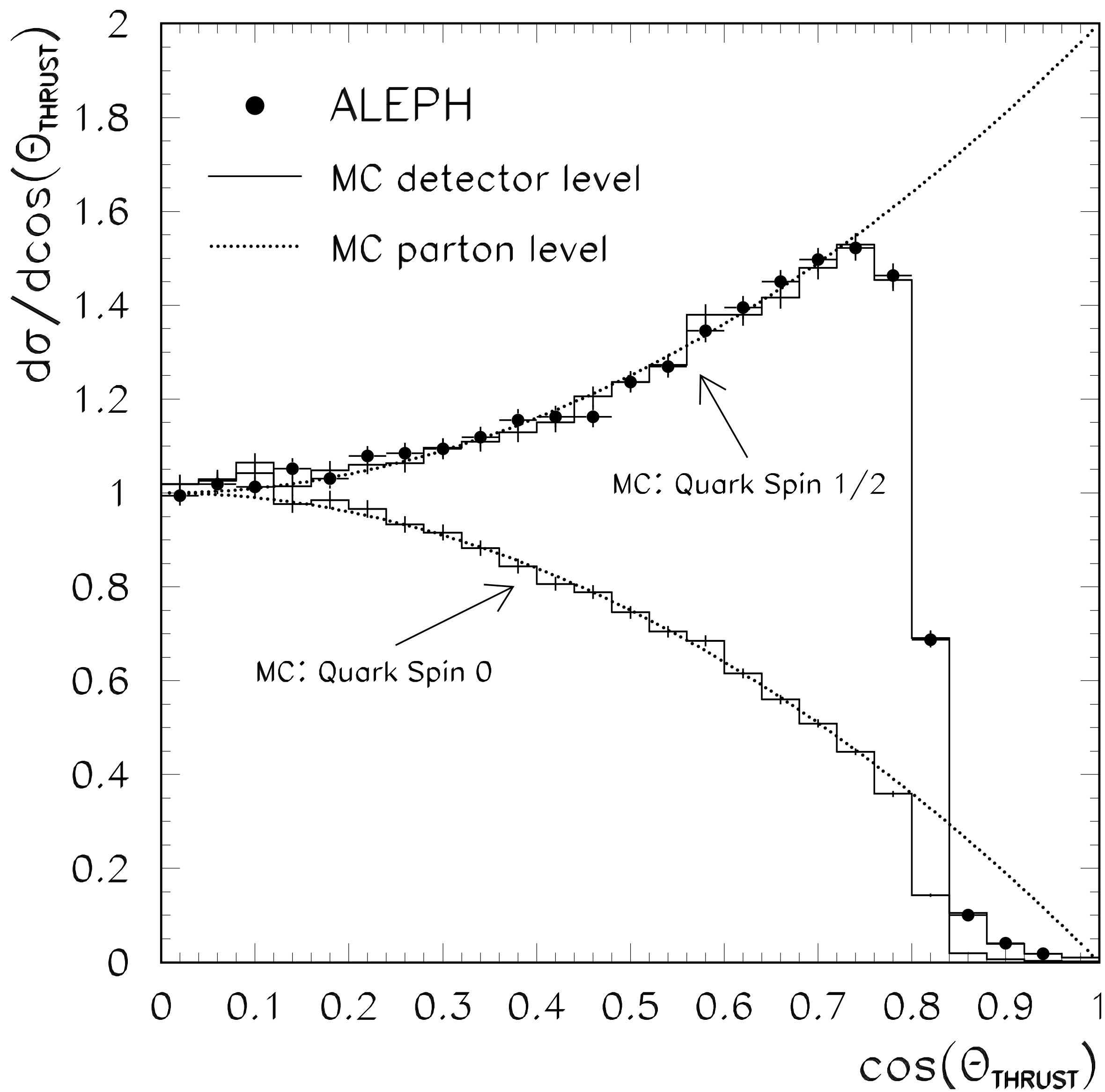

Figure 116: Angular distribution of the quark jet in e^+e^- annihilation, compared with models (ALEPH experiment at LEP, 1992-1994)

For a quark-antiquark pair,

$$\frac{d\sigma}{d\cos\theta}(e^+e^- \to q\bar{q}) = N_c e_q^2 \frac{d\sigma}{d\cos\theta}(e^+e^- \to \mu^+\mu^-) \qquad (135)$$

where the fractional charge of a quark e_q is taken into account and factor $N_c = 3$ is number of colours.

- Experimentally measured angular dependence is clearly proportional to $(1 + \cos^2\theta) \Rightarrow$ jets are aligned with spin-1/2 particles – quarks

- If a high-momentum (hard) gluon is emitted by a quark or antiquark, it fragments to a jet of its own, which leads to a three-jet event
  - Observation of three-jet events in e+e- annihilation at PETRA accelerator (DESY, Hamburg) in 1979 is credited as gluon discovery

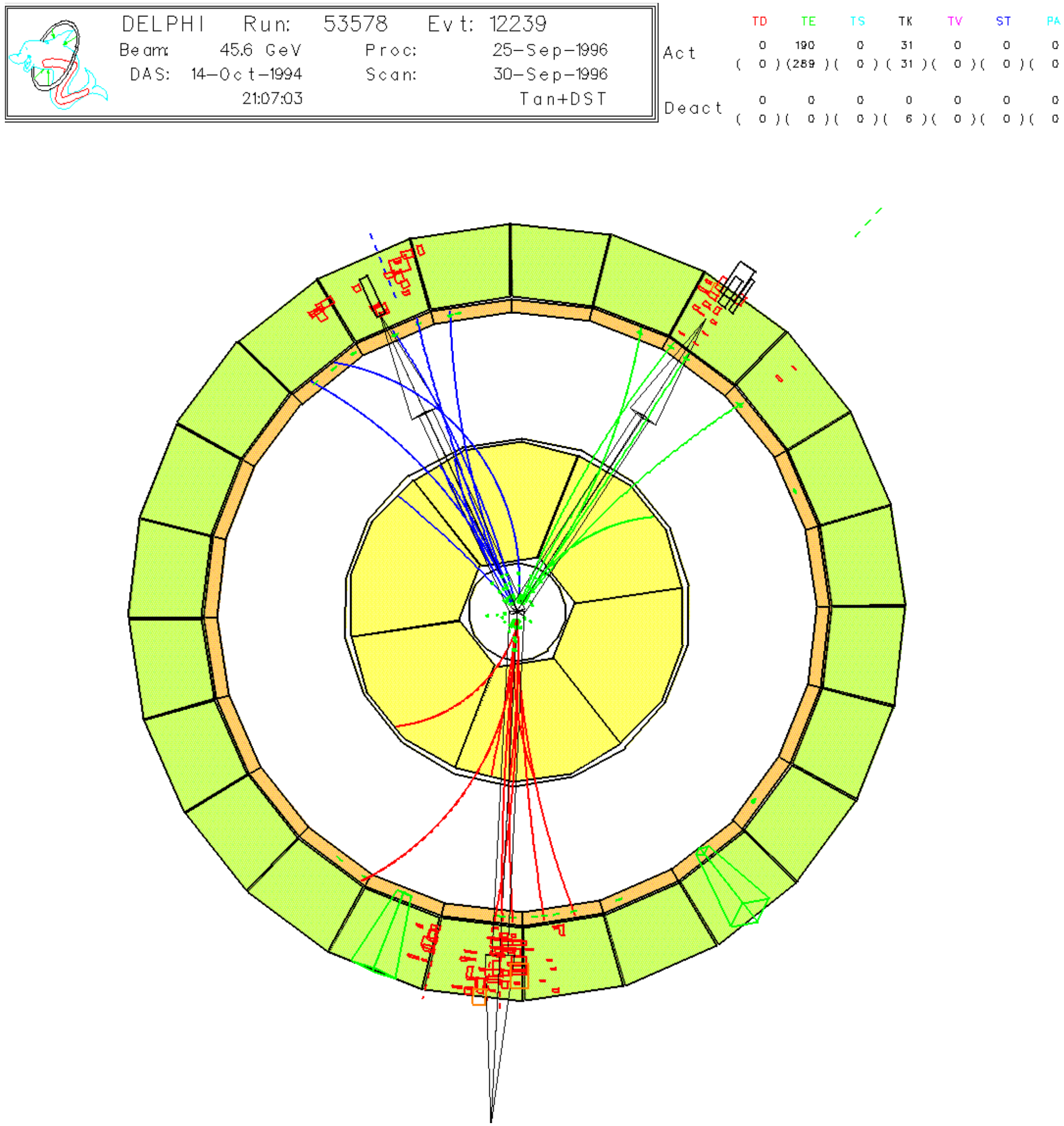

Figure 117: A three-jet event in e^+e^-annihilation as seen by the DELPHI experiment at LEP (1996)

- In three-jet events, it is difficult to distinguish which of the jets belongs to the gluon, hence a specific sensitive variable has to be chosen

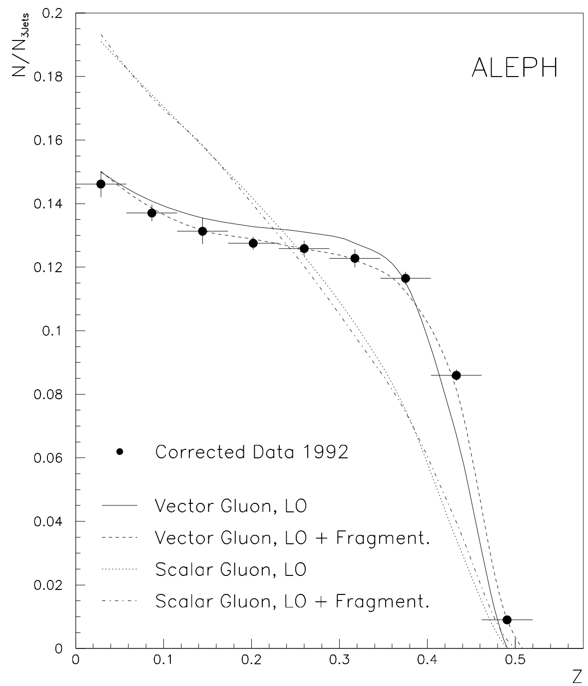

Figure 118: Distribution of Z (as in Eq.(136)) in 3-jet e^+e^- annihilation events, compared with models

- Jets are ranked by energies $E_1>E_2>E_3$ (E_1 ought to be a quark), and Z is:

$$Z = \frac{1}{\sqrt{3}}(E_2 - E_3) \tag{136}$$

- Angular distributions of jets confirm models where quarks are spin-1/2 fermions and gluons are spin-1 bosons

- Observed rate of three-jet to two-jet events can be used to determine value of α_s (probability for a quark to emit a gluon is determined by α_s):

$$\alpha_s = 0.15 \pm 0.03 \quad \text{for } E_{CM} = 30 \text{ to } 40 \text{ GeV (at PETRA)}$$

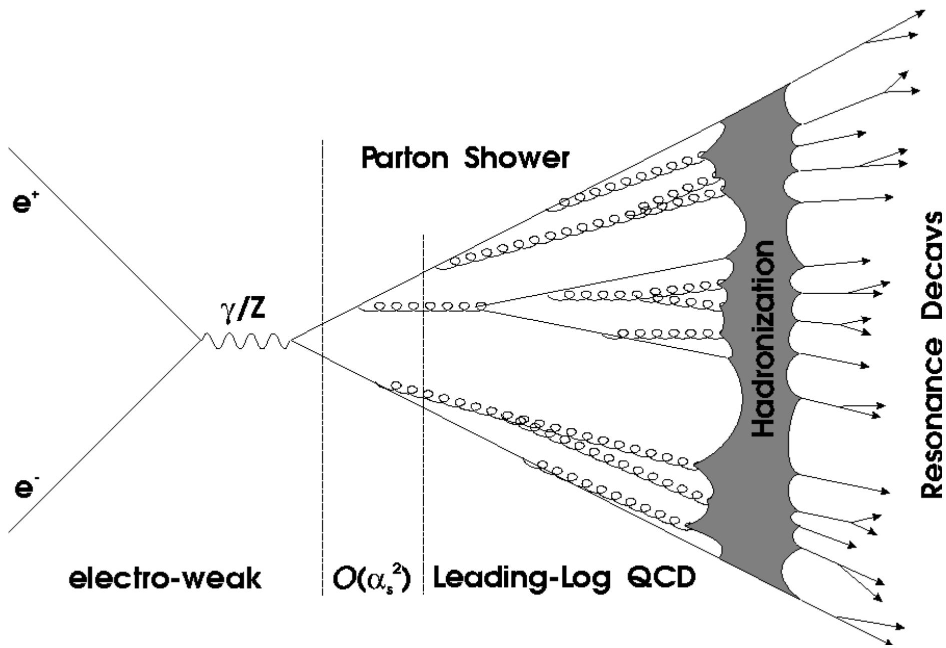

Figure 119: Principal scheme of hadroproduction in e^+e^- annihilation. Hadronization (=fragmentation) begins at distances of order 1 fm between partons

The *total cross-section* of $e^+e^- \to hadrons$ is often shown as in Eq.(105):

$$R \equiv \frac{\sigma(e^+e^- \to hadrons)}{\sigma(e^+e^- \to \mu^+\mu^-)} \tag{137}$$

where the denominator is (see also Eq.(106))

$$\sigma(e^+e^- \to \mu^+\mu^-) = \frac{4\pi\alpha^2}{3Q^2} \tag{138}$$

Using the same argumentation as in Eq.(135) and assuming that the main contribution comes from quark-antiquark two-jet events,

$$\sigma(e^+e^- \to hadrons) = \sum_q \sigma(e^+e^- \to q\bar{q}) = 3\sum_q e_q^2 \sigma(e^+e^- \to \mu^+\mu^-) \tag{139}$$

and hence

$$R = 3\sum_q e_q^2$$

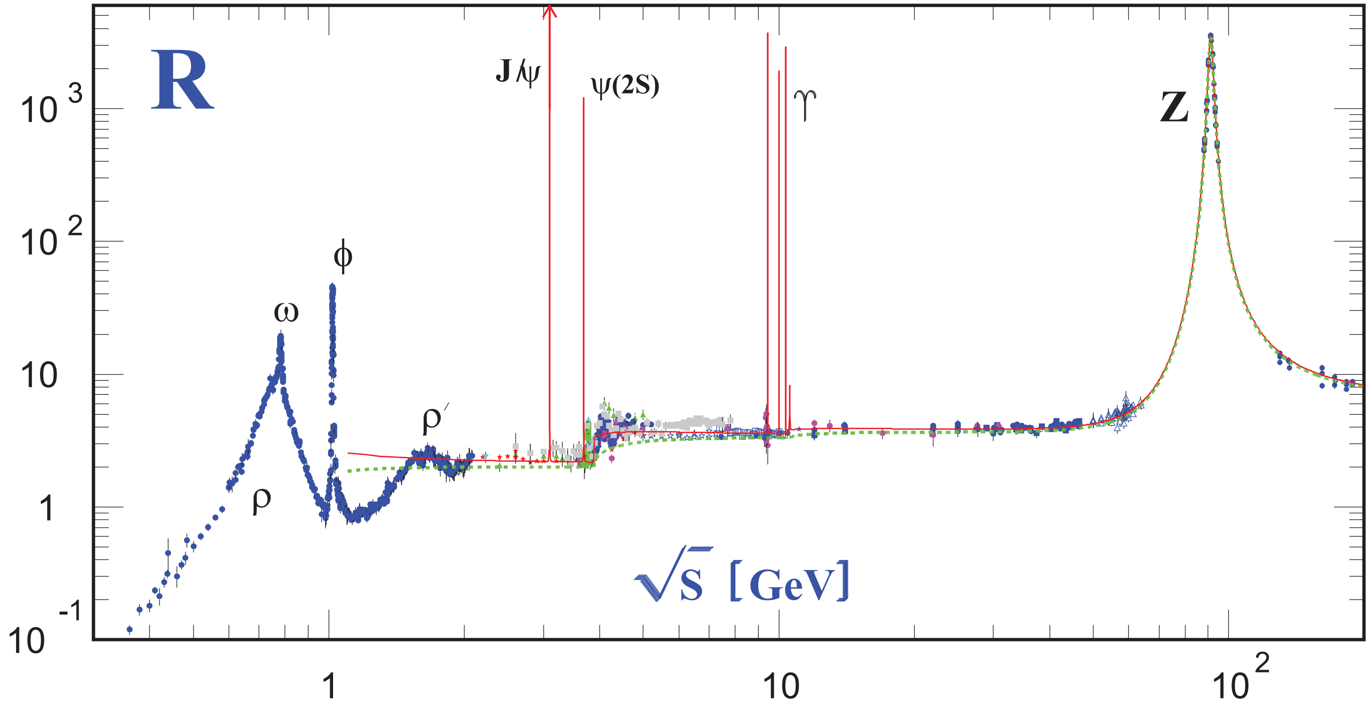

Figure 120: Measured R (Eq.(137)) with theoretical predictions for five available flavours (u,d,s,c,b), using two different α_s calculations

- R is a good probe for both number of colours in QCD and number of quark flavours allowed to be produced at a given Q: from Eq.(139) it follows that:

$$R(u,d,s)=2\ ;\ R(u,d,s,c)=10/3\ ;\ R(u,d,s,c,b)=11/3$$

If the radiation of hard gluons is taken into account, the extra factor proportional to α_s arises:

$$R = 3\sum_q e_q^2\left(1 + \frac{\alpha_s(Q^2)}{\pi}\right) \tag{140}$$

Elastic electron scattering off nucleons

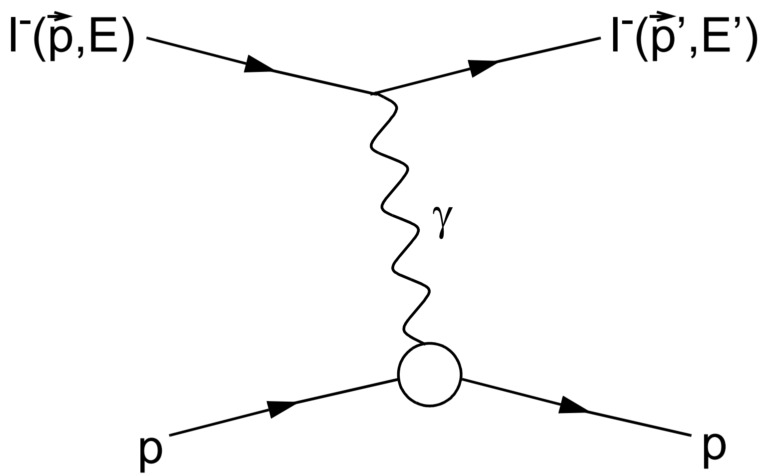

Figure 121: Dominant one-γ exchange process for elastic lepton-proton scattering

- Elastic scattering: particles nature does not change

Electron-proton scattering

Electrons are a good tool for investigating properties of hadrons, since electrons do not have a substructure. The wavelength of the exchanged photon determines how the hadron (usually, a proton) is being probed.

$\lambda >> r_p$ **Very low electron energies**

The scattering is equivalent to that from a "point-like" spin-less object.

$\lambda = r_p$ **Low electron energies**

The scattering is equivalent to that from an extended charged object.

$\lambda < r_p$ **High electron energies**

The wavelength is short enough to make it possible to interact with the valence quarks in the proton.

$\lambda << r_p$ **Very high electron energies**

The electron can at these short wavelengths interact with the sea of quarks and gluons.

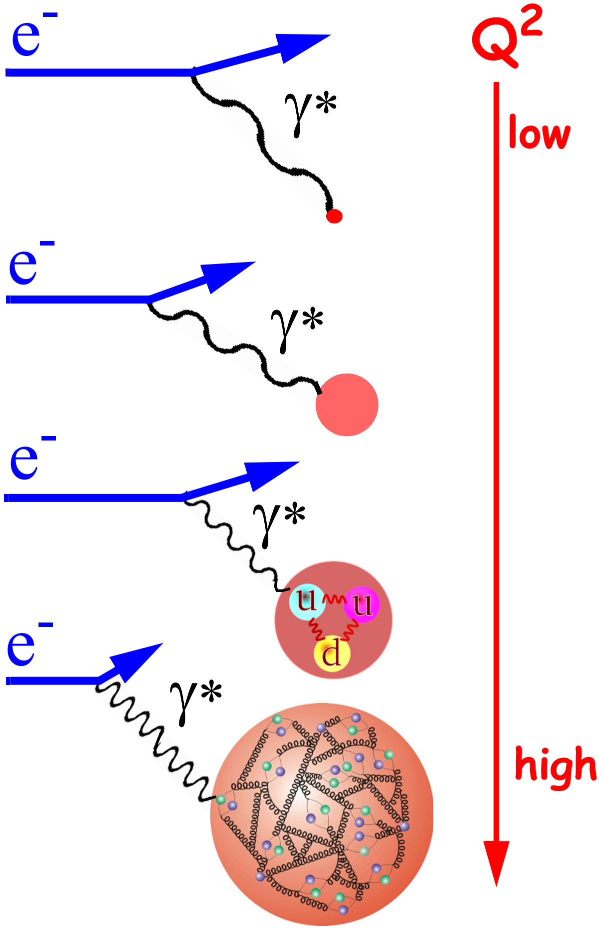

❖ Elastic lepton-hadron scattering has been used to measure sizes of hadrons

Angular distribution of a relativistic electron of momentum $p>>m$ scattered by a static electric charge e is described by the Mott formula:

$$\left(\frac{d\sigma}{d\Omega}\right)_M = \frac{\alpha^2}{4p^2 \sin^4(\theta/2)}\left(m^2 + p^2 \cos^2\frac{\theta}{2}\right) \qquad (141)$$

For non-relativistic electrons ($p \approx 0$), Rutherford formula is used:

$$\left(\frac{d\sigma}{d\Omega}\right)_R = \frac{m^2\alpha^2}{4p^2 \sin^4(\theta/2)} \qquad (142)$$

Here Ω is the solid angle of scattered electron, θ is its asimuthal angle, and $\alpha = e^2/4\pi$

If the electric charge is spread with a spherically symmetric density distribution, i.e., $e \to e\rho(r)$, where $\rho(r)$ is normalized: $\int \rho(r) d^3\vec{x} = 1$

then the differential cross-section (142) is replaced by

$$\frac{d\sigma}{d\Omega} = \left(\frac{d\sigma}{d\Omega}\right)_R G_E^2(q^2) \tag{143}$$

where the *electric form factor*

$$G_E(q^2) = \int \rho(r) e^{i\vec{q}\cdot\vec{x}} d^3\vec{x} \tag{144}$$

is the Fourier-transform of $\rho(r)$ with respect to the momentum transfer $\vec{q} = \vec{p} - \vec{p}'$.

– For $q = 0$, $G_E(0) = 1$ (low momentum transfer)

– For $q^2 \to \infty$, $G_E(q^2) \to 0$ (large momentum transfer)

- Measurements of the cross-section (143) determine the form-factor and hence the charge distribution inside the proton
  - If proton is an elementary particle without structure, $G_E = 1$ independently of q

For example, the RMS charge radius is given by

$$r_E^2 \equiv \overline{r^2} = \int r^2 \rho(r) d^3\vec{x} = -6 \left.\frac{dG_E(q^2)}{dq^2}\right|_{q^2 = 0} \tag{145}$$

- In addition to G_E, there is also G_M – the *magnetic form factor*, associated with the magnetic moment distribution within the proton
- At high momentum transfers, the *recoil energy* of the proton is not negligible, and $\vec{q}$ is replaced by the Lorentz-invariant Q
  - at high Q (non-relativistic electrons) static interpretation of charge and magnetic moment distribution breaks down
  - Eq.(145) is obviously valid only for low $Q^2 = q^2$

For a high-energy electron ($m << E$), and taking into account magnetic moment of the electron itself, one obtains:

$$\frac{d\sigma}{d\Omega} = \frac{\alpha^2}{4E^2 \sin^4(\theta/2)}\left(\frac{E'}{E}\right)\left[G_1(Q^2)\cos^2\left(\frac{\theta}{2}\right) + 2\tau G_2(Q^2)\sin^2\left(\frac{\theta}{2}\right)\right] \qquad (146)$$

Here E' is electron's energy after scattering, and

$$G_1(Q^2) = \frac{G_E^2 + \tau G_M^2}{1+\tau} \; ; \; G_2(Q^2) = G_M^2 \; ; \; \tau = \frac{Q^2}{4M_p^2}$$

and form factors are normalized so that

$$G_E(0) = 1 \;\; and \;\; G_M(0) = \mu_p = 2.79$$

- Experimentally, it is sufficient to measure E' and θ of outgoing electrons in order to derive G_E and G_M using Eq.(146)

Results of proton size measurements are conveniently divided into three Q^2 regions: low, intermediate and high

- low $Q^2 \Rightarrow \tau$ is very small $\Rightarrow G_E$ dominates the cross-section and r_E can be precisely measured:

$$r_E = 0.85 \pm 0.02\ fm \tag{147}$$

- intermediate range: $0.02 \le Q^2 \le 3\ \mathrm{GeV}^2 \Rightarrow$ both G_E and G_M give sizeable contribution $\Rightarrow$ they can be defined e.g. through a parameterization:

$$G_E(Q^2) \approx \frac{G_M(Q^2)}{\mu_p} \approx \left(\frac{\beta^2}{\beta^2 + Q^2}\right)^2 \tag{148}$$

with β^2=0.84 GeV

- high Q^2>3 $\mathrm{GeV}^2 \Rightarrow$ only G_M can be measured accurately

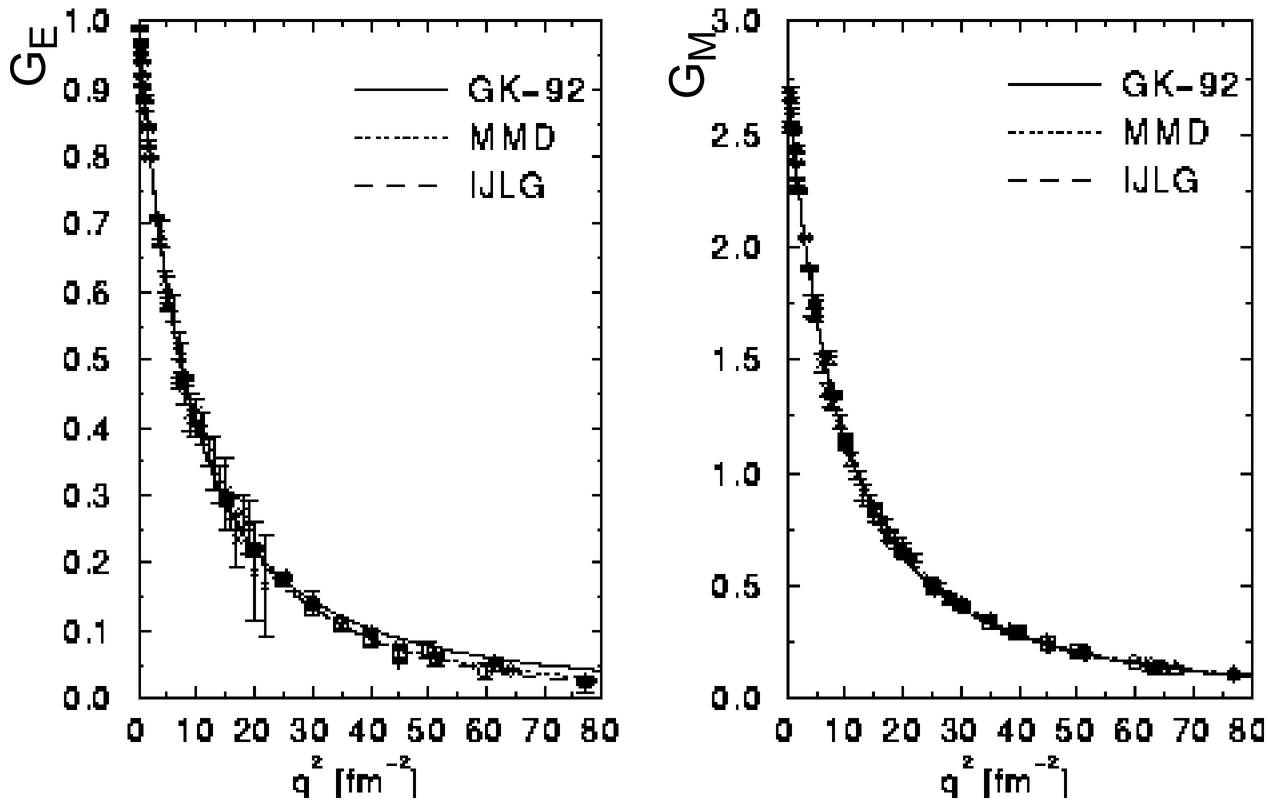

Figure 122: Electric and magnetic proton form-factors, compared with different parameterizations

- Such form-factor behaviour (e.g., $G_E \neq 1$) indicates that proton is **not** a point-like structure
  - For neutron, $G_E(0)=0$

Inelastic lepton scattering

- Historically, was first to give evidence of quarks in protons
  - In what follows, only one-photon exchange is considered

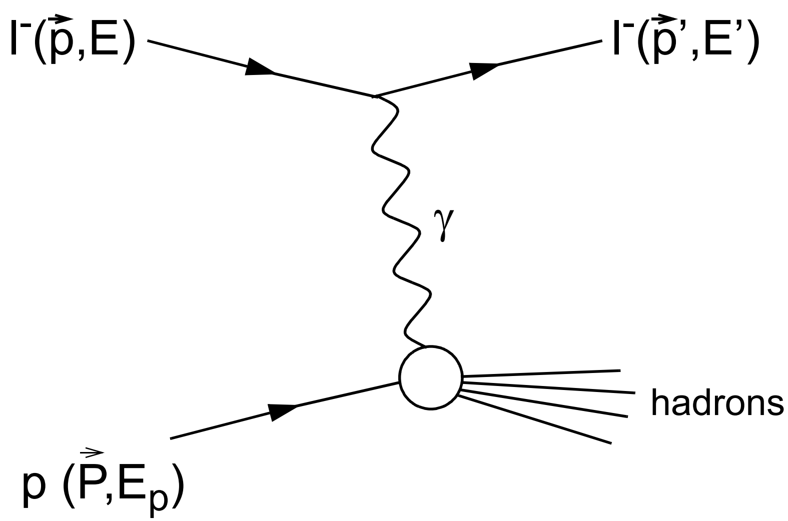

Figure 123: One-photon exchange in inelastic lepton-proton scattering

- The exchanged photon acts as a probe of the proton structure

- Momentum transfer $\vec{p}-\vec{p}'$ must be **big** enough to cause very **small** photon wavelength, small enough to probe a proton

While fixed-target experiments were the first, most profound studies were made on electron-proton colliders at SLAC and DESY:

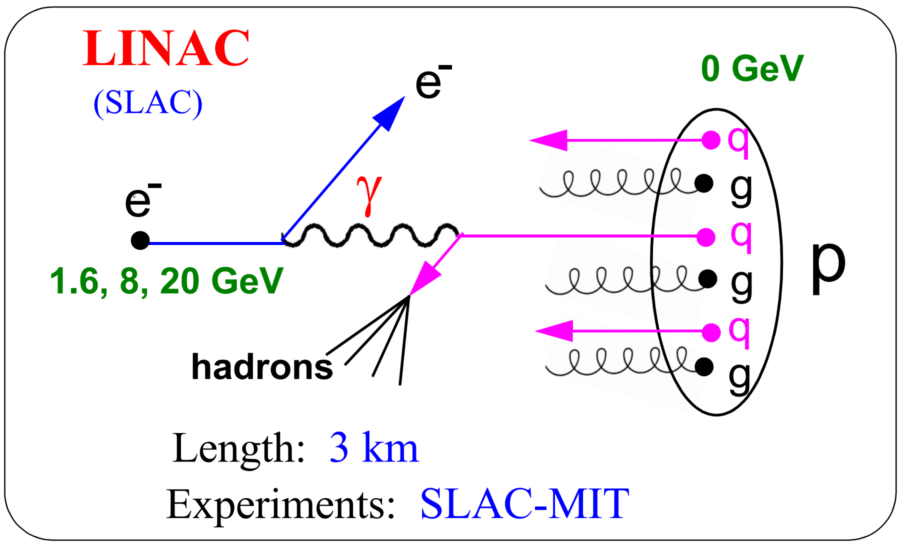

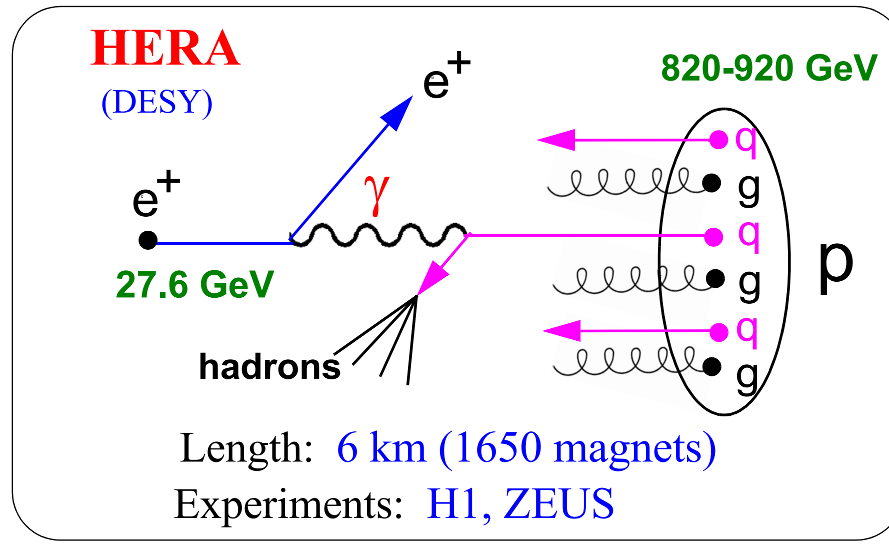

❖ When a photon resolves a quark within a proton, the total lepton-proton scattering is a two-step process:

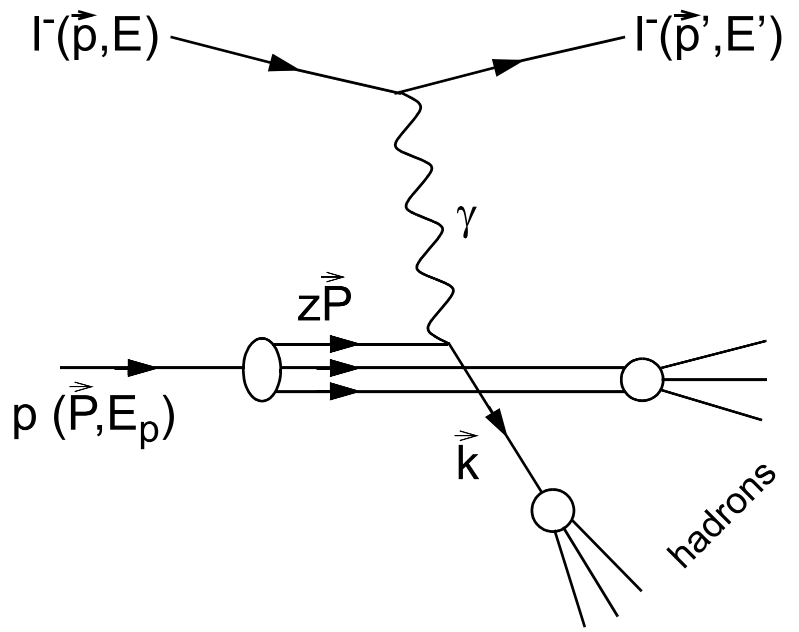

Figure 124: Detailed picture of deep-inelastic lepton-proton scattering

1) First step: elastic scattering of the lepton from one of the quarks:

$$l^- + q \to l^- + q \qquad (l = e,\ \mu)$$

2) Second step: fragmentation of the *recoil quark* and the proton remnant into observable hadrons

- Angular distributions of recoil leptons reflect properties of quarks from which they scattered

For further studies, some new variables have to be defined:

- Lorentz-invariant generalization for the transferred energy ν:

$$2M_p\nu \equiv W^2 + Q^2 - M_p^2 \tag{149}$$

where W is the invariant mass of the final hadron state; in the rest frame of the proton $\nu = E - E'$

- Dimensionless scaling variable x:

$$x \equiv \frac{Q^2}{2M_p\nu} \tag{150}$$

For $Q \gg M_p$ and a very large proton momentum $\vec{P} \gg M_p$, x is the *fraction* of the proton momentum carried by the struck quark; $0 \leq x \leq 1$

- Energy E' and angle θ of scattered lepton are independent variables, describing inelastic process

$$\frac{d\sigma}{dE'd\Omega'} = \frac{\alpha^2}{4E^2 sin^4\left(\frac{\theta}{2}\right)} \frac{1}{\nu}\left[cos^2\left(\frac{\theta}{2}\right)F_2(x, Q^2) + sin^2\left(\frac{\theta}{2}\right)\frac{Q^2}{xM_p^2}F_1(x, Q^2)\right] \quad (151)$$

  - Form (151) is a generalization of the elastic scattering formula (146)
  - *Structure functions* F_1 and F_2 parameterize the interaction at the quark-photon vertex (just like G_1 and G_2 parameterized the elastic scattering)

- *Bjorken scaling* (a.k.a *scale invariance*) was observed by many experiments:

$$F_{1,\,2}(x, Q^2) \approx F_{1,\,2}(x) \quad (152)$$

At $Q \gg M_p$, structure functions are approximately independent on Q^2.

  - Meaning: if all particle masses, energies and momenta are multiplied by a scale factor, structure functions at any given x remain unchanged

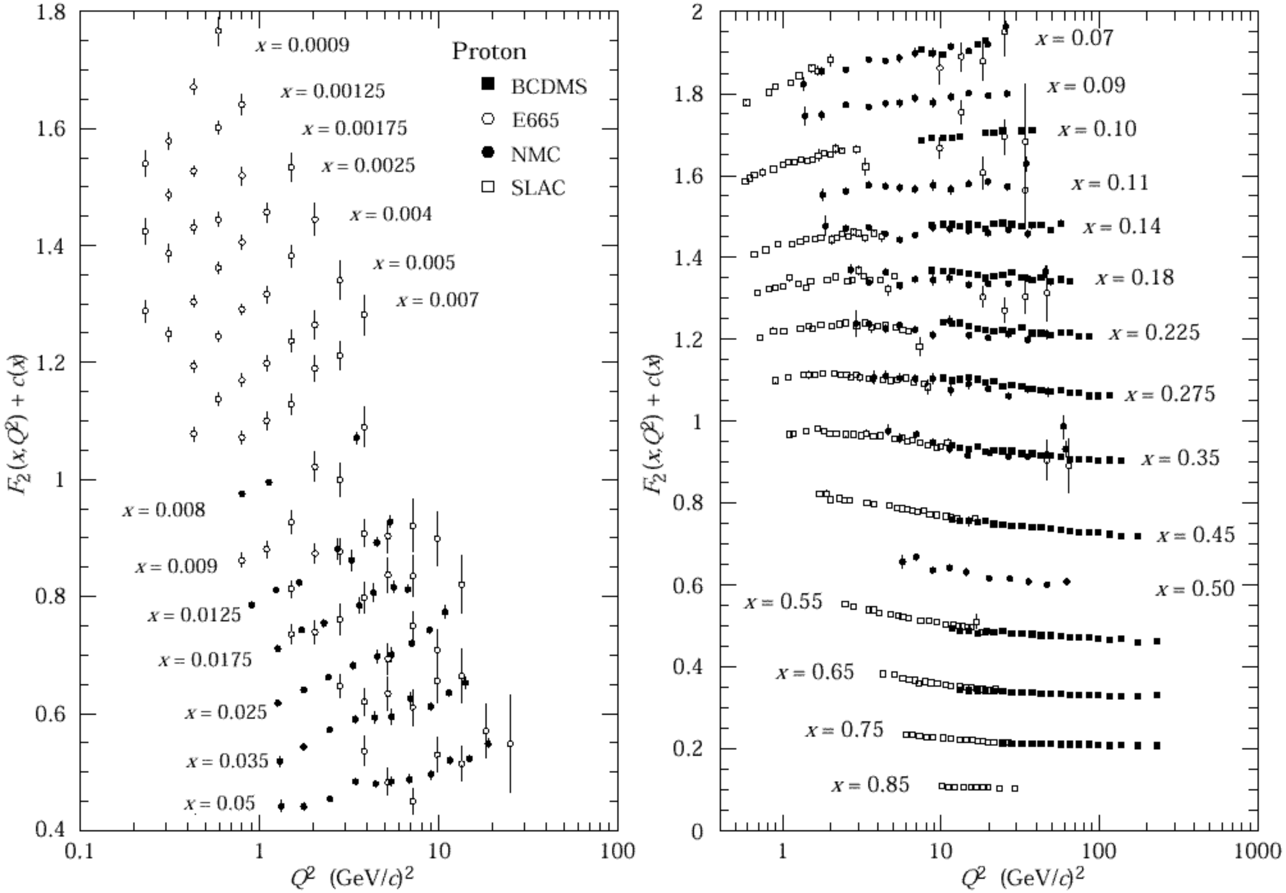

Figure 125: Structure functions F_2 of proton from different experiments

- SLAC data from 1969 were first evidence of *partons*

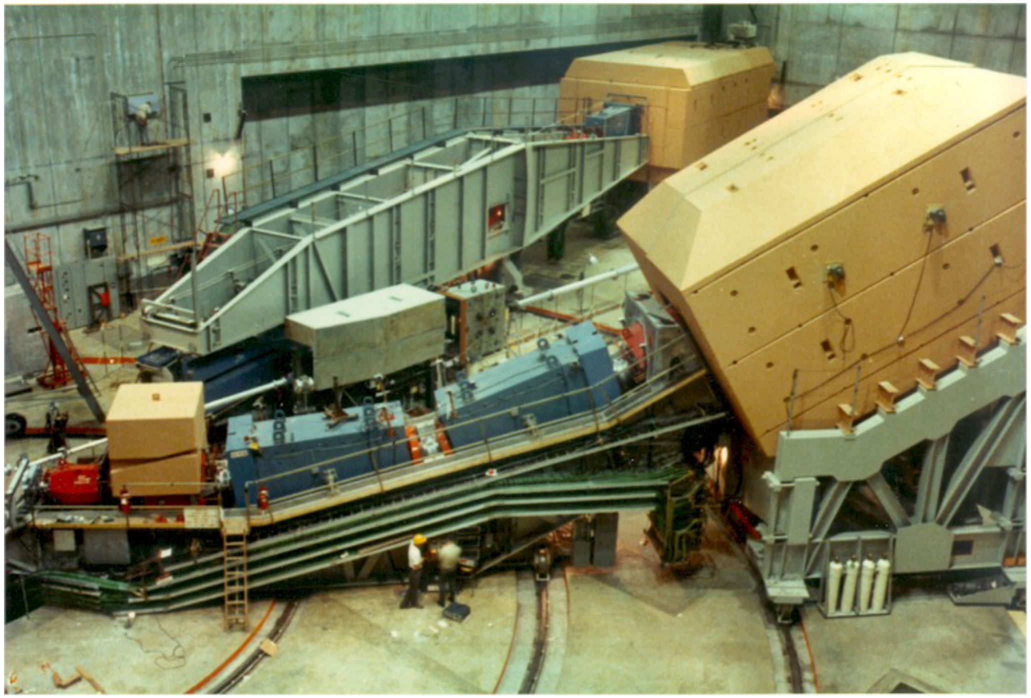

Figure 126: SLAC's End Station A: proton target (left) and spectrometers

- The observed approximate scaling behaviour can be explained if protons are considered as composite objects
  - *Scaling violation* is observed at very small and very big x: evidence of higher-order effects

- The trivial *parton model* assumes that proton consists of some partons; interactions between partons are not taken into account.
- Measured cross-section at any given x is proportional to the probability of finding a parton with a fraction $z=x$ of the proton momentum

If there are several partons,

$$F_2(x, Q^2) = \sum_a e_a^2 x f_a(x) \quad (153)$$

where $f_a(x)dx$ is the probability of finding parton a with fractional momentum between x and $x+dx$.

- Parton distributions $f_a(x)$ are not known theoretically $\Rightarrow$ $F_2(x)$ has to be measured experimentally
  - However, $f_a(x)$ are predicted to be the same for all Q^2

While form (153) does not depend on the spin of a parton, predictions for F_1 do:

$$\begin{aligned} F_1(x, Q^2) &= 0 && \textit{(spin-0)} \\ 2xF_1(x, Q^2) &= F_2(x, Q^2) && \textit{(spin-1/2)} \end{aligned} \tag{154}$$

- The expression for spin-1/2 is called *Callan-Gross relation* and is very well confirmed by experiments ⇒ most evidently partons are quarks (!)
- Comparing proton and neutron structure functions and those from neutrino scattering, squared charge e_a^2 of Eq.(153) can be evaluated; it appears to be consistent with square charges of quarks.